N-myc coordinates retinal growth with eye size during mouse development

Rodrigo A.P. Martins,[1] Frederique Zindy,[2] Stacy Donovan,[1] Jiakun Zhang,[1] Stanley Pounds,[3] Alice Wey,[4,5] Paul S. Knoepfler,[4,5] Robert N. Eisenman,[6] Martine F. Roussel,[2] and Michael A. Dyer[1,7,8]

[1]Department of Developmental Neurobiology, St. Jude Children's Research Hospital, Memphis, Tennessee 38105, USA; [2]Department of Genetics and Tumor Cell Biology, St. Jude Children's Research Hospital, Memphis, Tennessee 38105, USA; [3]Department of Biostatistics, St. Jude Children's Research Hospital, Memphis, Tennessee 38105, USA; [4]Department of Cell Biology and Human Anatomy, University of California at Davis, Davis, California 95616, USA; [5]Institute for Pediatric Regenerative Medicine, Shriners Hospitals for Children, Sacramento, California 95817, USA; [6]Division of Basic Sciences, Fred Hutchinson Cancer Research Center, Seattle, Washington 98109, USA; [7]Department of Ophthalmology, University of Tennessee Health Science Center, Memphis, Tennessee 38163, USA

Myc family members play crucial roles in regulating cell proliferation, size, differentiation, and survival during development. We found that N-myc is expressed in retinal progenitor cells, where it regulates proliferation in a cell-autonomous manner. In addition, N-myc coordinates the growth of the retina and eye. Specifically, the retinas of *N-myc*-deficient mice are hypocellular but are precisely proportioned to the size of the eye. N-myc represses the expression of the cyclin-dependent kinase inhibitor p27Kip1 but acts independently of cyclin D1, the major D-type cyclin in the developing mouse retina. Acute inactivation of *N-myc* leads to increased expression of p27Kip1, and simultaneous inactivation of *p27Kip1* and *N-myc* rescues the hypocellular phenotype in *N-myc*-deficient retinas. N-myc is not required for retinal cell fate specification, differentiation, or survival. These data represent the first example of a role for a Myc family member in retinal development and the first characterization of a mouse model in which the hypocellular retina is properly proportioned to the other ocular structures. We propose that N-myc lies upstream of the cell cycle machinery in the developing mouse retina and thus coordinates the growth of both the retina and eye through extrinsic cues.

[*Keywords*: Cell cycle; proliferation; p27Kip1; cyclin D1; proto-oncogene]

Supplemental material is available at http://www.genesdev.org.

Received August 23, 2007; revised version accepted November 14, 2007.

A series of complex developmental processes must be carefully orchestrated for the vertebrate eye to form correctly. For example, retinal progenitor cell proliferation is coordinated with cell fate specification to ensure that each retinal cell type is produced in the correct proportion at the appropriate developmental stage (Cepko et al. 1996; Dyer and Cepko 2001a; Livesey and Cepko 2001). In addition, retinal progenitor cell proliferation must be coordinated with the growth of the other ocular structures to ensure that the retina has the proper dimensions for the size of the eye. One important aspect of this coordination is that retinal thickness is conserved across species, irrespective of eye size. For example, the volume of the mouse eye is ~5000 times smaller than that of the elephant eye, but the retinal thickness in these two species is comparable (Glickstein and Millodot 1970). Virtually nothing is known about the molecular mechanisms that regulate eye growth in concert with retinal growth to produce a retina that is proportioned to the size of the eye.

Genetically engineered mice have provided valuable insight into the molecular mechanisms that regulate retinal progenitor cell proliferation during development, but they have provided few clues about the coordination of retinal growth and eye size. One reason for this is that in most genetically engineered mice with hypocellular retinas, retinal progenitor cell proliferation and eye growth are uncoupled. For example, *Chx10*-deficient mice have small eyes with hypocellular retinas that are much too thin for the size of the eye; thus, the mice are blind (Burmeister et al. 1996); *cyclin D1*-knockout mice have a similar phenotype (Ma et al. 1998). To the best of our knowledge, no gene has been shown to regulate vertebrate retinal progenitor cell proliferation and maintain the normal coordination of retinal growth and eye size.

N-myc is a member of a family of proto-oncogenes

[8]**Corresponding author.**
E-MAIL michael.dyer@stjude.org; FAX (901) 495 3143.
Article is online at http://www.genesdev.org/cgi/doi/10.1101/gad.1608008.

(*Myc*, *Mycn*, *Mycl1*) encoding basic helix–loop–helix leucine-zipper (bHLHZ) transcription factors that regulate gene expression through a variety of mechanisms (for reviews, see Eisenman 2001; Zeller et al. 2003; Cole and Nikiforov 2006; Kleine-Kohlbrecher et al. 2006;). Myc family members play crucial roles in regulating the proliferation, size, differentiation, and survival of cells during development (for review, see Grandori et al. 2000). *N-myc*-deficient embryos die in utero due to developmental defects, and N-myc has been implicated in the development of the nervous system (Charron et al. 1992; Stanton et al. 1992; Davis et al. 1993).

In addition to their important roles in normal development, Myc family members, when inappropriately expressed, can lead to cancer in a variety of tissues (Nesbit et al. 1999; Lutz et al. 2002). Misexpression of N-myc is often associated with pediatric neural cancers such as neuroblastoma, medulloblastoma, and retinoblastoma (Brodeur et al. 1984; Lee et al. 1984; Choi et al. 1993; Aldosari et al. 2002; Hatton et al. 2006; MacPherson et al. 2007).

To study the role of N-myc in retinal development, we analyzed eyes from *Nestin-Cre;N-myc*$^{Lox/Lox}$ mice (Tronche et al. 1999; Knoepfler et al. 2002). *Nestin-Cre* is expressed in retinal progenitor cells (MacPherson et al. 2004); thus, it is an ideal experimental system to study the role of N-myc in retinal development. Inactivation of *N-myc* in retinal progenitor cells caused decreased proliferation and a hypocellular retina. No perturbations in retinal cell fate specification, differentiation, survival, or cell size occurred in the absence of N-myc. The p27Kip1 cyclin-dependent kinase inhibitor (CKI) was up-regulated upon *N-myc* inactivation, and simultaneous inactivation of *N-myc* and *p27Kip1* rescued the defect in retinal progenitor cell proliferation. In addition, we found that the size of the eye is smaller in *Nestin-Cre; N-myc*$^{Lox/Lox}$ mice, although N-myc expression in the nonretinal structures of the eyes was not perturbed. Indeed, we found that the eyes of *Nestin-Cre; N-myc*$^{Lox/Lox}$ mice were precisely proportioned to the size of the retina such that the proper retinal thickness was preserved. These data suggest that N-myc is upstream of the key regulatory pathways that coordinate retinal growth with eye growth during development and provide the first insight into this complex regulatory process.

Results

Expression of the Myc family during retinal development

To determine when Myc family members (N-myc, c-myc, and L-myc) are expressed during retinal development, we searched the mouse retina SAGE library (Blackshaw et al. 2001; http://itstgp01.med.harvard.edu/retina). Expression of *N-myc* and that of *c-myc* were found as early as embryonic day 12.5 (E12.5), and the level of *N-myc* expression was at least three times higher than that of *c-myc* at all developmental stages analyzed (Fig. 1A; Supplemental Fig. 1A). Expression of both genes was detected through postnatal stages, with no detectable tags in adult retinas. No tags for *L-myc* were detected at any stage of retinal development (data not shown). To verify these SAGE data, we performed real-time PCR with TaqMan probes specific for *N-myc* and *c-myc* on cDNA prepared from seven stages of mouse retinal development (E14.5, E17.5, postnatal day 0 [P0], P3, P6, P12, and adult) (Fig. 1B; Supplemental Fig. 1B). Consistent with the SAGE data, *N-myc* and *c-myc* were expressed at their highest levels during embryonic and postnatal retinal development (E14.5–P6) (Fig. 1B; Supplemental Fig. 1B). A sharp decrease in the expression of *N-myc* and *c-myc* was observed in adult retinas (P30), when all retinal progenitor cell proliferation had ceased (Fig. 1B). To measure N-myc protein expression during retinal development, we immunoblotted retinal lysates at five stages of retinal development (E14.5, P0, P6, P12, and adult) (Fig. 1C). Those results were consistent with the SAGE and real-time RT–PCR analyses. In situ hybridization revealed that *N-myc* and *c-myc* are expressed by retinal progenitor cells at E14.5 and P0 and by post-mitotic differentiated cells in E17, P0, P6, and adult retina (Fig. 1D; Supplemental Fig. 1C).

N-myc*-deficient retinas are hypocellular*

To study the role of N-myc in retinogenesis, we analyzed the eyes of *Nestin-Cre; N-myc*$^{Lox/Lox}$ mice (Tronche et al. 1999; Knoepfler et al. 2002). In these animals, Cre recombinase is broadly expressed in progenitor cells of the developing CNS, including the retina (Graus-Porta et al. 2001; MacPherson et al. 2004). Comparison of eyes from *Nestin-Cre; N-myc*$^{Lox/Lox}$ mice (referred to as *N-myc*$^{-/-}$ or *N-myc*-deficient) and their control littermates (*N-myc*$^{Lox/Lox}$; referred to as control) revealed that the *N-myc*-deficient retinas were smaller (Fig. 1, F vs. E). To measure the retinal volume, we serially sectioned control and *N-myc*-deficient adult retinas, traced each section using BioQuant 5.0 software, and generated a three-dimensional reconstruction (Fig. 1G,H). The volume of the *N-myc*-deficient retinas was significantly smaller than that of the control retinas ($P = 0.015$) (Fig. 1I). Eye size did not correlate with body weight, indicating that the phenotype was specific for the cells expressing *Nestin-Cre* in the developing retina (data not shown). Next, we dissociated retinas from *N-myc*-deficient mice and control littermates and scored the total number of cells per retina. Consistent with the reduced retinal volume, we found that the *N-myc*-deficient retinas were hypocellular ($P = 0.009$) (Fig. 1J). The cell density of *N-myc*-deficient retinas was indistinguishable from that of their control littermates (Fig. 1K), suggesting that there was no difference in cell size in the absence of *N-myc*.

N-myc *regulates retinal progenitor cell proliferation*

A previous report suggested that the anatomical defects observed in *N-myc*-deficient cerebella are in part caused

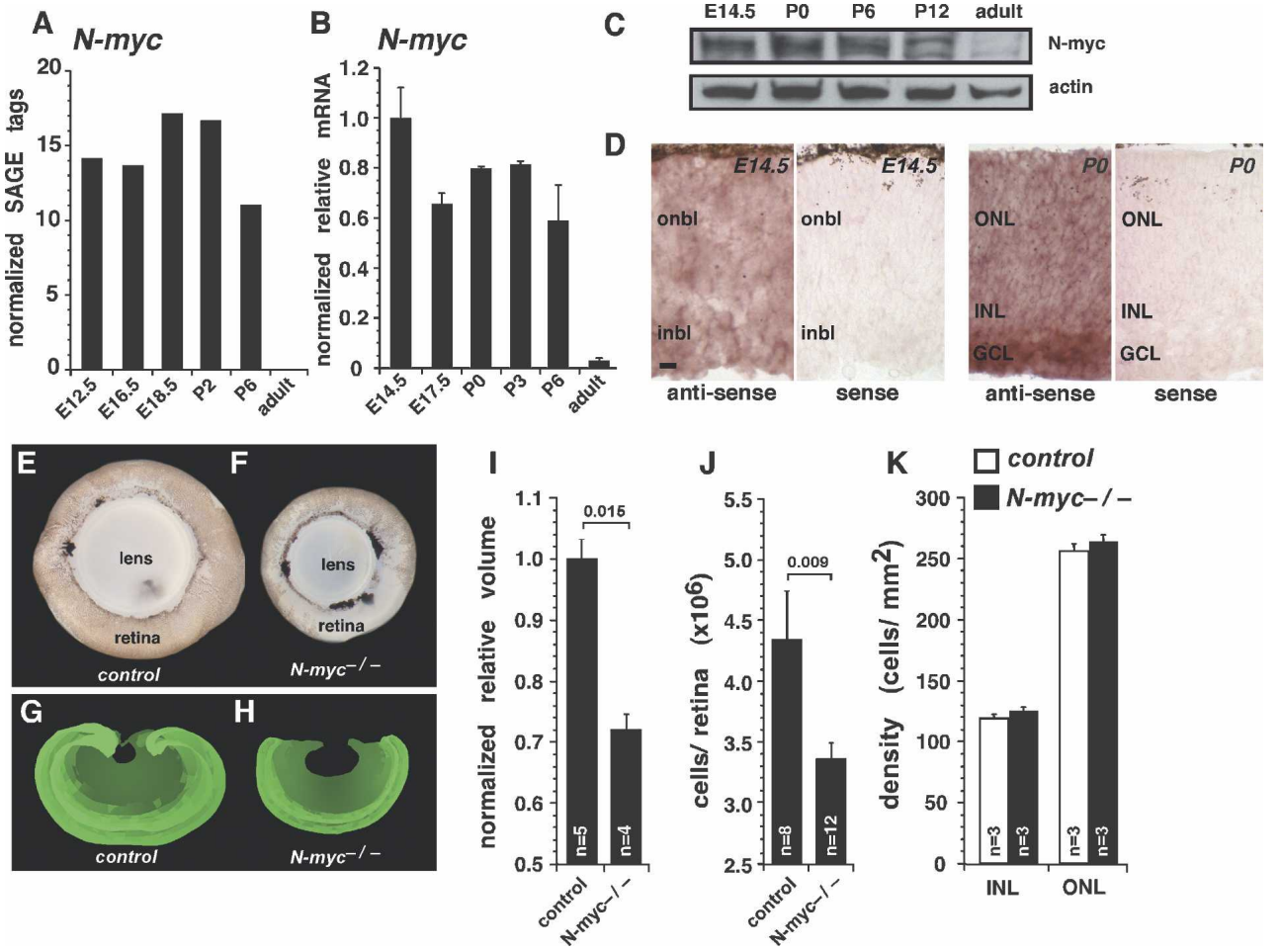

Figure 1. *N-myc*-deficient retinas are smaller and contain fewer cells. SAGE (*A*) and real-time RT–PCR (*B*) analyses of *N-myc* mRNA expression at six stages of mouse retinal development. Real-time RT–PCR data were obtained using TaqMan probes, and data sets ($n = 4$) were normalized to *Gapdh* (*Gapd*) expression. Normalized relative expression shows that *N-myc* expression is highest in the embryonic retina and decreases as development proceeds. (*C*) Western blot analysis of N-myc protein expression during retinal development confirmed the mRNA expression data. (*D*) In situ hybridization analysis revealed that *N-myc* is expressed in retinal progenitor cells and post-mitotic cells of developing retinas. (*E,F*) Eyes from adult control (*N-myc*$^{Lox/Lox}$) and *N-myc*-deficient retina (*Nestin-Cre; N-myc*$^{Lox/Lox}$) mice were dissected with the lens intact. (*G,H*) Representative control and *N-myc*-deficient sections of retinas that were reconstructed using BioQuant 5.0 software to measure retinal volume. (*I*) *N-myc*-deficient retinas were significantly smaller than controls. (*J*) Individual *N-myc*-deficient and control retinas were dissociated, and total cell numbers were scored. *N-myc*-deficient retinas had fewer cells than did controls. (*K*) Cell density in the inner nuclear layer and outer nuclear layer was measured in *N-myc*-deficient (filled bars) and control (open bars) retinas. No difference was found in the inner nuclear layer ($P = 0.4$) or outer nuclear layer ($P = 0.2$). (onbl) Outer neuroblastic layer; (inbl) inner neuroblastic layer; (ONL) outer nuclear layer; (INL) inner nuclear layer; (GCL) ganglion cell layer. Error bars indicate SEM. Bar: *D*, 10 μm.

by a decreased pool of neuroepithelial progenitor cells in the rhombic lip (Knoepfler et al. 2002). To test whether the starting population of retinal progenitor cells is affected by conditional inactivation of *N-myc* in the developing CNS, we measured the volume of E12.5 *N-myc*-deficient retinas in serial sections and compared those data with that from control littermates. At E12.5, there was no significant difference in the volumes of the retinas (Fig. 2A). However, by P0, the *N-myc*-deficient retinas were smaller than the control retinas (Fig. 2B), and this persisted through the later stages of retinal development, including P6, P15, and adult (Figs. 2C, 1E,F, 4G [below]; data not shown). These data suggest that the hypocellular phenotype of *N-myc*-deficient retinas may be caused by a progenitor cell proliferation defect rather than a defect in optic cup formation.

To directly analyze the proliferation and clonal expansion of individual retinal progenitor cells over the course of retinal development, we infected E14.5 retinas from *Nestin-Cre; N-myc*$^{Lox/Lox}$ embryos or control littermates with the NIN-E retrovirus (Dyer and Cepko 2001b). This replication-incompetent retrovirus only infects proliferating retinal progenitor cells and expresses nuclear LacZ, which is ideal for scoring clone size (Fig. 2D–F). After 10 d in culture, the retinas were fixed and stained with X-gal to label the cells infected with the NIN-E retrovirus.

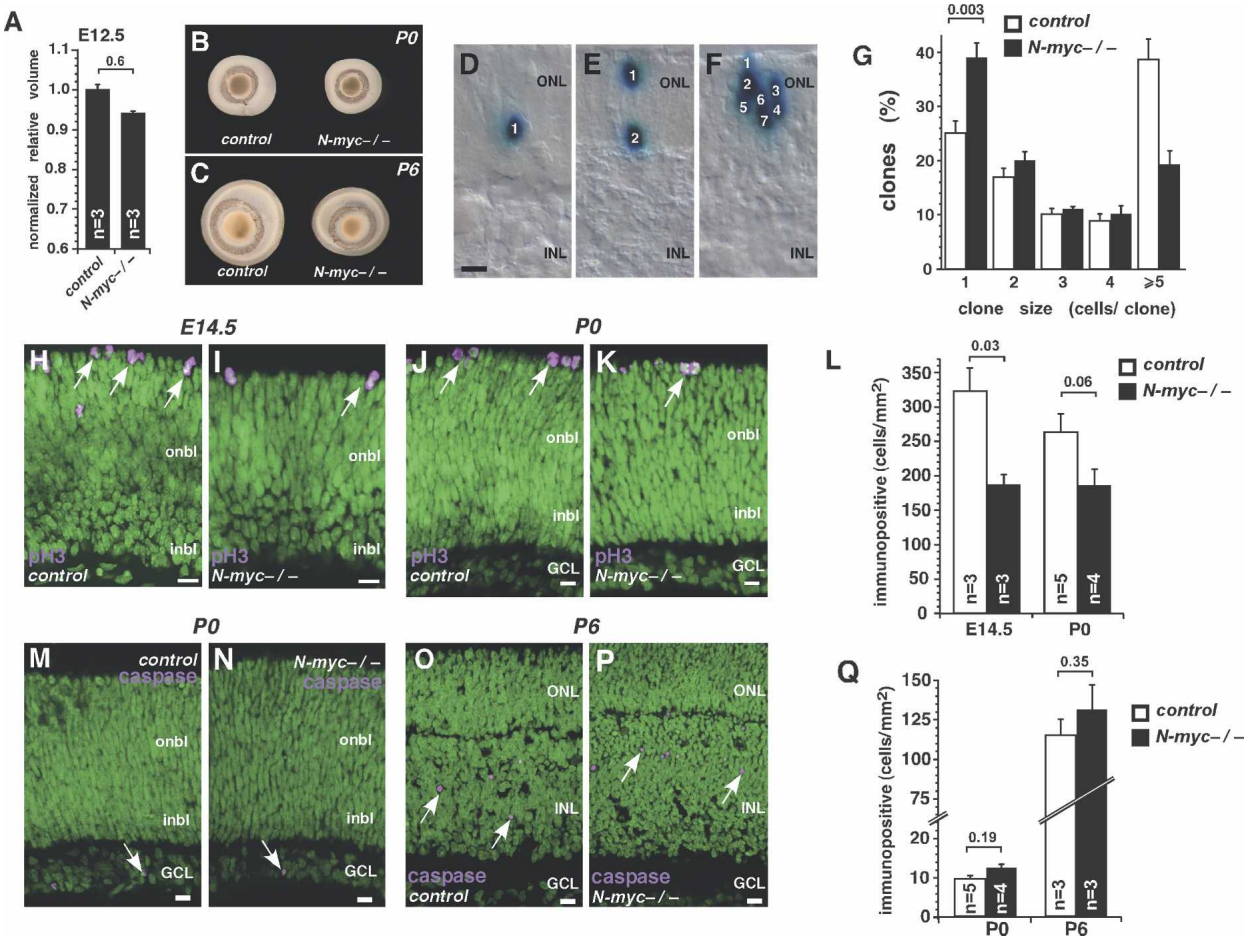

Figure 2. N-myc regulates retinal progenitor cell proliferation. (*A*) *N-myc*-deficient and control retinas from E12.5 mice were sectioned and reconstructed to obtain volume measurements using BioQuant 5.0. No significant difference in retinal volume was observed at E12.5 ($P = 0.6$). (*B*,*C*) Representative pictures from P0 (*B*) and P6 (*C*) control and *N-myc*-deficient dissected eyes. (*D–F*) Representative pictures of clones of cells derived from infection of individual retinal progenitor cells with the NIN-E retrovirus. The NIN-E retrovirus encodes nuclear LacZ, which allows the quantification of clone size, a measure of retinal progenitor cell proliferation during development. (*G*) E14.5 retinas from control (open bars; $n = 8$) and *N-myc*-deficient (filled bars; $n = 8$) mice were infected with NIN-E and maintained in culture as whole-tissue explants for 10 d. Clone size was scored on serial sections of each retina. In the absence of N-myc, the proportion of one-cell clones increased at the expense of large clones (five or more cells). (*H–K*) Representative confocal pictures of pH3 immunostaining of control (*H*,*J*) and *N-myc*-deficient (*I*,*K*) retinas at E14.5 (*H*,*I*) and P0 (*J*,*K*). (*L*) Quantification of pH3$^+$ cells per area in control (open bars) and *N-myc*-deficient (filled bars) retinas at E14.5 and P0. (*M–P*) Representative confocal pictures of activated caspase-3 immunostaining of control (*M*,*O*) and *N-myc*-deficient (*N*,*P*) retinas at P0 (*M*,*N*) and P6 (*O*,*P*). (*Q*) Quantification of activated caspase-3$^+$ cells per area in control (open bars) and *N-myc*-deficient (filled bars) retinas. (onbl) Outer neuroblastic layer; (inbl) inner neuroblastic layer; (ONL) outer nuclear layer; (INL) inner nuclear layer; (GCL) ganglion cell layer. Error bars indicate SEM. Bars, 10 µm.

Clones were reconstructed from serial sections, and the number of cells in each clone was scored. More than 600 total clones were scored for each genotype. Consistent with a defect in retinal progenitor cell proliferation, we found a significant increase in the proportion of one-cell clones ($P = 0.003$) and a decrease in the proportion of large clones (five or more cells) in *N-myc*-deficient retinas as compared with controls (Fig. 2G). Similar results were obtained from P0 retinas (data not shown).

To test whether *N-myc* loss affected retinal progenitor cell proliferation in vivo, we scored the proportion of phospho-histone H3 (pH3)-immunopositive cells at E14 and P0 in *N-myc*-deficient and control retinas (Fig. 2H–K). The pH3 immunoreactivity is found in retinal progenitor cells during the M phase of the cell cycle. *N-myc*-deficient retinas had fewer pH3$^+$ cells at E14.5 and P0 than did controls (Fig. 2L). Similar results were observed for other markers of proliferating cells, such as Ki67 (Supplemental Fig. 2).

Together, the pH3 data and the lineage analysis suggest that proliferation is reduced in *N-myc*-deficient retinas. However, it is possible that apoptosis increases during retinal development in the absence of N-myc, and this, in turn, reduces the proportion of dividing cells (ElShamy et al. 1998; Wartiovaara et al. 2002; Okubo et al. 2005). To test this directly, we scored the proportion

of activated caspase-3-immunopositive cells in *N-myc*-deficient and control retinas at E17.5, P0, P3, and P6. No difference in the proportion or the localization of activated caspase-3$^+$ cells was observed at any stage examined (Fig. 2M–Q; data not shown).

N-myc regulates retinal progenitor cell proliferation in a cell-autonomous manner

To determine if N-myc regulates retinal progenitor cell proliferation in a cell-autonomous manner, we inactivated *N-myc* in individual retinal progenitor cells by using two different approaches. In the first experiment, E17.5 *N-myc*$^{Lox/Lox}$ retinas were square-wave-electroporated with plasmids expressing Cre-recombinase and a venus-YFP reporter (vYFP) gene (Fig. 3A). As a control, the contralateral eye was electroporated with a plasmid expressing vYFP. Retinal explants were maintained in culture for 48 h (Donovan and Dyer 2006) to allow sufficient time for Cre-mediated recombination of the *N-myc*^{Lox} allele (Fig. 3A; Schweers and Dyer 2005). Next, the S-phase cells in the retinal explants were pulse-labeled with bromodeoxyuridine (BrdU) for 1 h. Culture media was changed and 23 h later, the retinal explants were labeled a second time with [^{3}H]-thymidine for 1 h to detect the cells that had progressed through the cell cycle and re-entered the S phase. Previous studies demonstrated that 24 h is sufficient time for retinal progenitor cells to progress through the cell cycle (Alexiades and Cepko 1996). Immediately after the [^{3}H]-thymidine pulse, the retinal explants were dissociated, and the vYFP-expressing cells were purified by FACS (Fig. 3B). These cells were then plated on glass slides, immunostained for BrdU, and overlaid with autoradiographic emulsion to detect the [^{3}H]-thymidine. The proportion of [^{3}H]-thymidine$^+$ cells and that of BrdU$^+$; [^{3}H]-thymi-

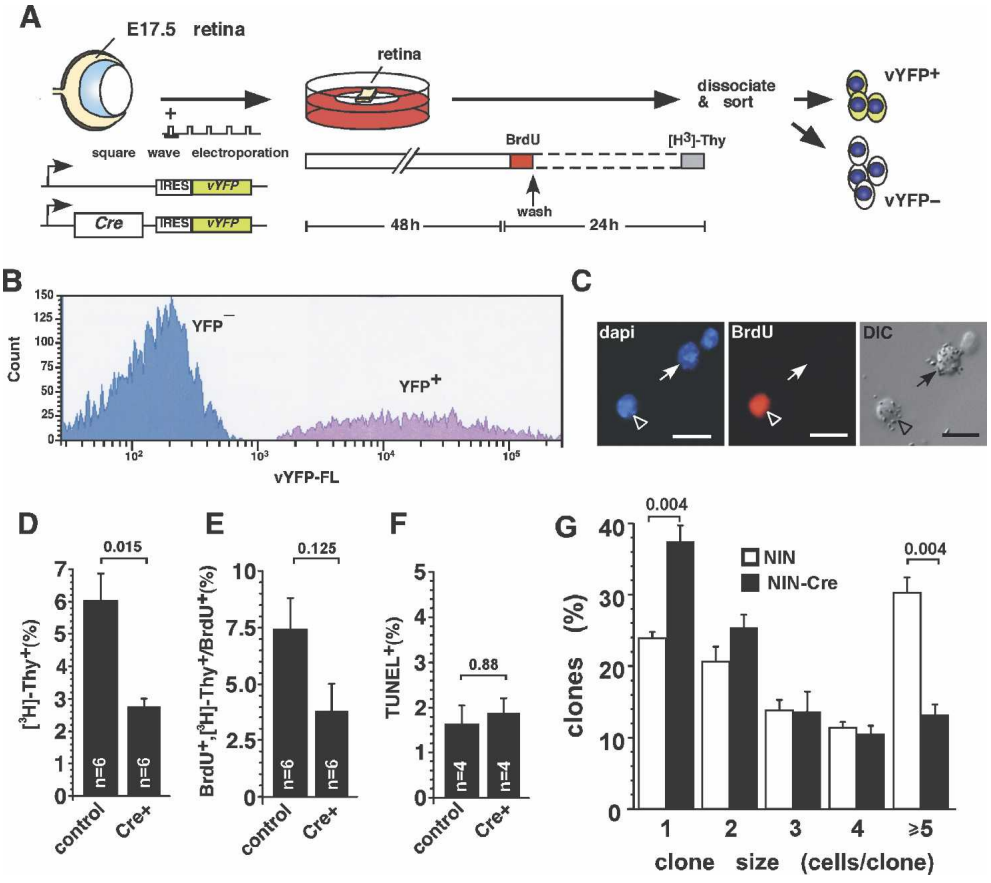

Figure 3. Acute gene inactivation reveals that N-myc has a cell-autonomous role in retinal progenitor cell proliferation. (*A*) E17.5 *N-myc*$^{Lox/Lox}$ retinas were square-wave-electroporated with a plasmid expressing Cre recombinase and a YFP reporter and then maintained in culture for 2 d. The YFP reporter plasmid was used as a control. S-phase cells were labeled by adding BrdU (10 µM) to the culture medium for 1 h. Explants were then washed and the culture medium was changed. (*B*) One day later, retinal explants were pulsed with [^{3}H]-thymidine for 1 h. Retinal cells were dissociated, and YFP$^+$ cells were purified by FACS. (*C*) Sorted retinal cells were plated, stained for BrdU (red), and overlaid with autoradiographic emulsion. DAPI nuclear counterstaining is shown in blue. Proportions of [^{3}H]-thymidine$^+$ cells (*D*), double-positive BrdU$^+$/[^{3}H]-thymidine$^+$ cells among BrdU$^+$ cells (*E*), and TUNEL$^+$ cells (*F*) in each sample were scored. Acute inactivation of *N-myc* reduced the proportion of proliferating cells with no effect on apoptosis. (*G*) E14.5 *N-myc*$^{Lox/Lox}$ retinas were infected with either the NIN-E retrovirus (open bars; $n = 9$) or the NIN-Cre retrovirus (filled bars; $n = 9$) that inactivates N-myc only in infected cells. All of the surrounding cells contained *N-myc*^{Lox} alleles that were not recombined. Clone size was reduced in the absence of N-myc. Bars, 10 µm.

dine$^+$ cells were scored in the retinas electroporated with either Cre/vYFP or vYFP alone (Fig. 3C). Acute inactivation of *N-myc* significantly reduced the proportions of [^{3}H]-thymidine$^+$ cells ($P = 0.015$) (Fig. 3D) and BrdU$^+$/[^{3}H]-thymidine$^+$ cells (Fig. 3E). These data are consistent with the reduction in the proportion of pH3$^+$ cells and the smaller clone size in *N-myc*-deficient retinas (Fig. 2). No difference was observed in the proportion of TUNEL$^+$ apoptotic cells between samples electroporated with Cre/vYFP and those electroporated with vYFP alone (Fig. 3F).

In a second experiment, we infected N-myc$^{Lox/Lox}$ retinas with the NIN-Cre retrovirus. In this experiment, only the infected cells were *N-myc*-deficient; therefore, we followed the clonal expansion of *N-myc*-deficient retinal progenitor cells among control progenitor cells. As a control, the NIN-E retrovirus was used for the contralateral retinas. Analysis of 1882 clones from nine independent retinas revealed that *N-myc*-deficient clones were smaller, as represented by a significant decrease in the proportion of large clones ($P = 0.004$) and an increase in the proportion of small clones ($P = 0.004$) compared with those in controls (Fig. 3G).

N-myc acts independently of cyclin D1 in the developing retina

Cyclin D1 is the major D-type cyclin expressed in the developing mouse retina (Sicinski et al. 1995; Dyer and Cepko 2001b). Previous studies have suggested that N-myc-mediated regulation of cerebellar granule cell proliferation occurs through the control of D-type cyclin expression (Kenney et al. 2003). To determine whether the reduction in retinal progenitor cell proliferation in the absence of N-myc was mediated by changes in cyclin D1 levels, we analyzed cyclin D1 expression by real-time RT–PCR and immunoblot analyses. There was no significant difference in the expression of cyclin D1 mRNA or protein in purified *N-myc*-deficient retinal cells (Fig. 4A,B).

To provide additional evidence that N-myc regulates retinal progenitor cell proliferation independent of cyclin D1, we analyzed the retinal volume of *cyclin D1*$^{-/-}$ and *Nestin-Cre*, *N-myc*$^{Lox/Lox}$*;cyclin D1*$^{-/-}$ mice. If the reduction in proliferation of retinal progenitor cells in *N-myc*-deficient retinas was caused by a decrease in cyclin D1 expression, then we would expect that the double-knockout retinas (*Nestin-Cre*, *N-myc*$^{Lox/Lox}$*;cyclin D1*$^{-/-}$) would be indistinguishable from the *cyclin D1*-deficient retinas, because according to this model, *cyclin D1* would be genetically downstream from *N-myc*. Alternatively, if N-myc acts independently of cyclin D1, then we predict that the *N-myc;cyclin D1*-deficient retinas would be smaller than the *cyclin D1*-deficient retinas because of the additive effect of inactivating these two important regulators of retinal progenitor cell proliferation.

The *cyclin D1*-deficient retinas were smaller than the *N-myc*-deficient retinas, and inactivation of both genes was additive, thus reducing retinal volume even more (Fig. 4C–F). Measurements of total retinal volume from three-dimensional reconstruction of serial sections confirmed that the simultaneous inactivation of *N-myc* and *cyclin D1* resulted in smaller retinas compared with either single-knockout retinas (Fig. 4G). The previously observed holes in the photoreceptor layer of *cyclin D1*-deficient retinas (Ma et al. 1998) were also observed in *Nestin-Cre*, *N-myc*$^{Lox/Lox}$*; cyclin D1*$^{-/-}$ retinas (Fig. 4H,I). This finding suggests that N-myc is not required for this phenotype.

N-myc regulates p27Kip1 expression in the mouse retina

In the N-myc-deficient cerebellum, the CKIs p27Kip1 and p18Ink4c are up-regulated and contribute to the hypocellular cerebellum (Knoepfler et al. 2002; Zindy et al. 2006). In addition, p27Kip1 and p19Ink4d are the major CKIs expressed during retinogenesis (Levine et al. 2000; Dyer and Cepko 2001b; Cunningham et al. 2002). To test whether N-myc regulates the expression of these two CKIs in the developing retina, we performed real-time RT–PCR and immunoblot analyses in control and *N-myc*-deficient retinal cells. Following acute *N-myc* inactivation, the expression of *p27Kip1* mRNA increased approximately twofold, but that of *p19Ink4d* did not change (Fig. 5A). The protein level of p27Kip1 also increased in the *N-myc*-deficient retinal cells (Fig. 5B).

To extend these findings, we generated double-knockout mice to determine whether simultaneous inactivation of *p27Kip1* and *N-myc* could restore the normal cell number in the *N-myc*-deficient retinas. Retinas from *Nestin-Cre;N-myc*$^{Lox/Lox}$*; p27Kip1*$^{-/-}$ mice contained the normal number of cells (Fig. 5C,D), and *Nestin-Cre;N-myc*$^{Lox/Lox}$*;p19Ink4d*$^{-/-}$ retinas were indistinguishable from *Nestin-Cre;N-myc*$^{Lox/Lox}$ retinas (Fig. 5C,D). We also performed clonal analysis with the NIN-E retrovirus in E14.5 *Nestin-Cre;N-myc*$^{Lox/Lox}$, *Nestin-Cre;N-myc*$^{Lox/Lox}$*; p27Kip1*$^{-/-}$, and control littermates. The clonal expansion of individual retinal progenitor cells was significantly increased in *N-myc;*

Table 1. *Retinal progenitor cells clone distribution in N-myc/CKI-deficient mice*

Cells per clone	Control	*N-myc*$^{-/-}$	*N-myc*$^{-/-}$*; p27*$^{-/-}$
1	25.1 ± 2.6% (378/1421)	39.1 ± 2.8% (350/896)	23.9 ± 2.3% (318/1371)
2–4	36.0 ± 1.9% (515/1421)	41.3 ± 1.8% (362/896)	40.6 ± 3.3% (537/1371)
≥5	38.9 ± 3.7% (532/1421)	19.6 ± 2.5% (184/896)	35.6 ± 4.6% (516/1371)

Statistics in Figure 5G.

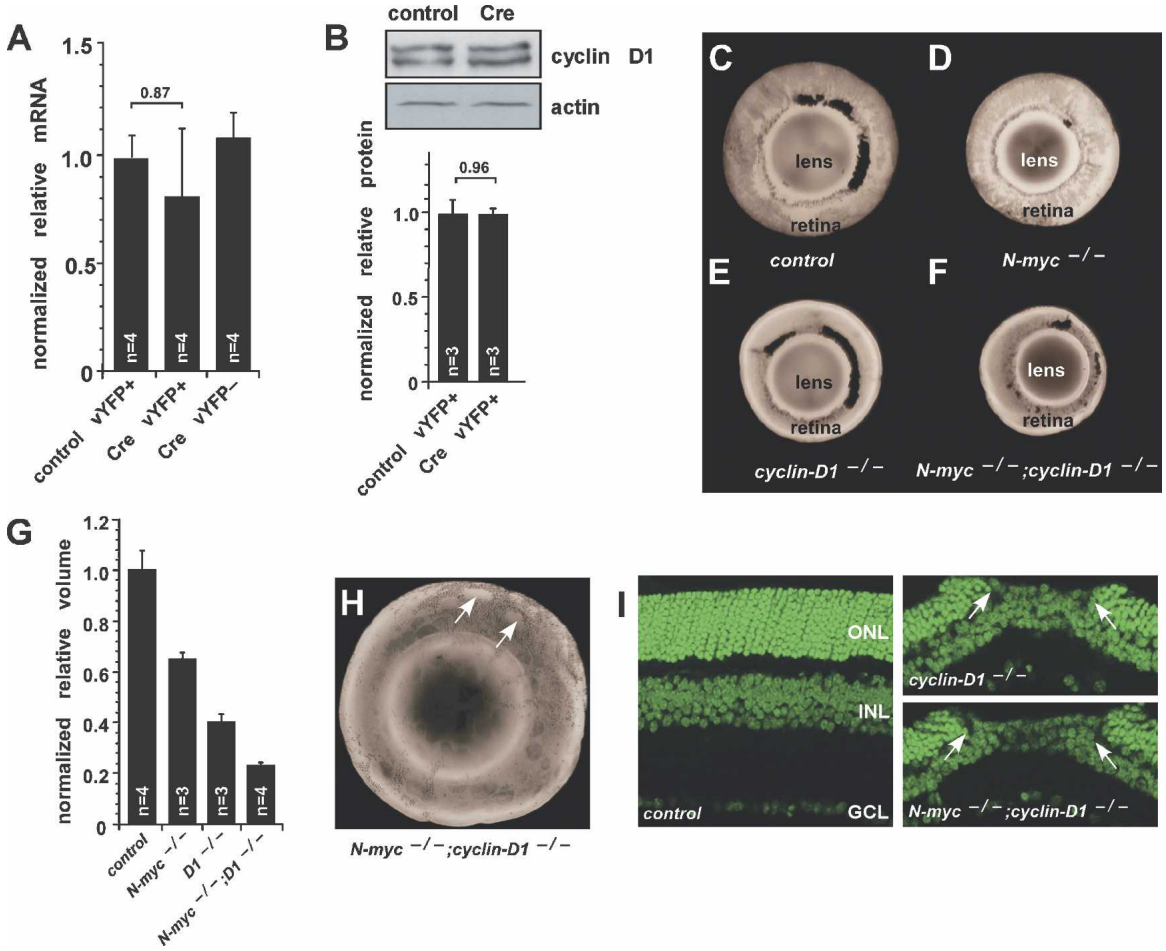

Figure 4. N-myc does not regulate *cyclin D1* expression in developing retinas. (*A*) E17.5 *N-myc*$^{Lox/Lox}$ retinas were square-wave-electroporated with either a control vector or a vector expressing Cre and then maintained in culture for 3 d. YFP^{+} cells were purified by FACS, and gene expression was analyzed by real-time RT–PCR. Samples were analyzed in duplicate and normalized to Gapdh (*Gapd*) expression. No difference in the level of expression of *cyclin D1* was observed after acute inactivation of N-myc. (*B*) A representative immunoblot shows that acute inactivation of N-myc does not affect cyclin D1 protein expression. (*C–F*) Representative pictures of dissected eyes from P15 control (*N-myc*$^{Lox/Lox}$) (*C*), *N-myc*-deficient (*Nestin-Cre, N-myc*$^{Lox/Lox}$) (*D*), *cyclin D1*-deficient (*cyclin D1*$^{-/-}$) (*E*), and double-deficient (*Nestin-Cre, N-myc*$^{Lox/Lox}$*;cyclin D1*$^{-/-}$) (*F*) mice. (*G*) Retinal volumes were measured by reconstructing serial sections using BioQuant 5.0 software. Simultaneous inactivation of *cyclin D1* and *N-myc* reduced retinal volume. (*H,I*) Retinas deficient in both *N-myc* and *cyclin D1* also displayed photoreceptor degeneration (arrows) as described for *cyclin D1*-deficient retinas. Error bars indicate SEM.

p27Kip1-deficient retinas compared with *N-myc*-deficient retinas (Fig. 5G; Table 1).

To provide additional evidence for a role of N-myc in regulating *p27Kip1* gene expression, we used a luciferase reporter construct that was fused to the mouse *p27Kip1* promoter (Yang et al. 2001). The p27Kip1–luciferase plasmid was square-wave-electroporated into P0 *N-myc*$^{Lox/Lox}$ retina along with a vYFP reporter gene and a plasmid that expressed Cre recombinase. In the contralateral retina, the vYFP reporter gene and the p27Kip1–luciferase plasmid were introduced. Forty-eight hours later, the luciferase expression was measured. There was a significant increase in p27Kip1–luciferase expression in the absence of *N-myc* (Fig. 5H). Similarly, when N-myc was ectopically expressed with the p27Kip1–luciferase reporter in the developing retina, the level of luciferase expression significantly decreased (Fig. 5I).

N-myc is not required for neuronal differentiation in the retina

To test whether retinal cell fate specification and differentiation proceed normally in the absence of N-myc, we analyzed the proportion and distribution of each class of retinal cell type in the *N-myc*-deficient retinas and the controls. Cone photoreceptors (cone arrestin) (Fig. 6A), amacrine cells (Pax6) (Fig. 6B), horizontal cells (calbindin) (Fig. 6C), rod photoreceptors (rhodopsin and recoverin) (Fig. 6D), Müller glia (glutamine synthetase and CD44) (Fig. 6E; data not shown), bipolar cells (Chx10 and PKCα) (Fig. 6F; data not shown), and ganglion cells (Gap43) (data not shown) were distributed normally in *Nestin-Cre; N-myc*$^{Lox/Lox}$ adult retinas. Dissociated cell scoring confirmed that the proportion of each cell type in *N-myc*-deficient retinas was similar to that in control

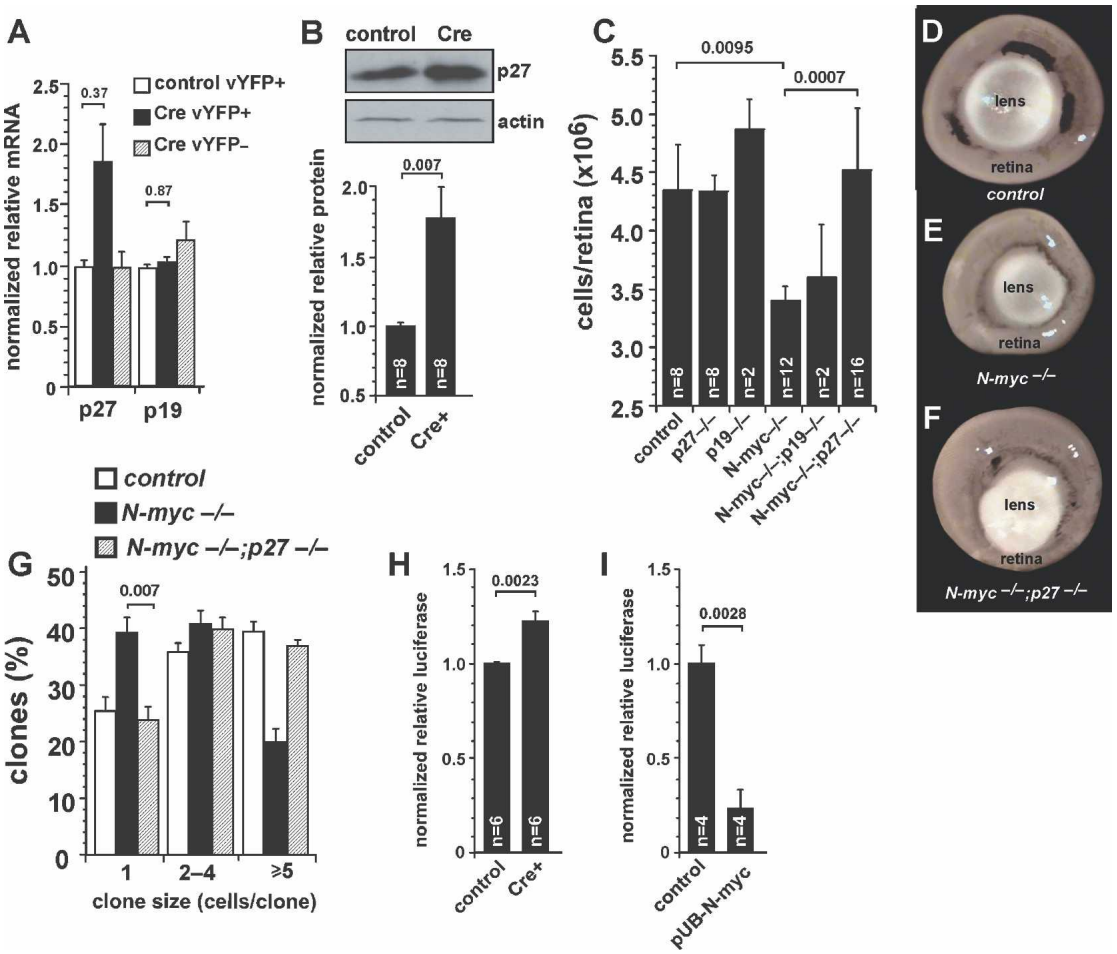

Figure 5. Inactivation of *p27Kip1* rescues progenitor cell proliferation defects in *N-myc*-deficient retinas. (*A*) E17.5 *N-myc*$^{Lox/Lox}$ retinas were square-wave-electroporated with either a control vector (open bars; $n = 4$) or a vector expressing Cre and then maintained in culture for 3 d. YFP$^+$ cells (filled bars; $n = 4$) were purified from YFP$^-$ cells (striped bars; $n = 4$) by FACS, and gene expression was analyzed by real-time RT–PCR. Samples were analyzed in duplicate and normalized to Gapdh (*Gapd*) expression. (*B*) A representative immunoblot shows expression of p27Kip1 protein. Acute inactivation of N-myc increased p27Kip1 mRNA and protein expression. (*C*) P30 retinas of various genotypes were dissociated, and total cell numbers were quantified. Inactivation of *p27Kip1* rescued the reduction in cell number of *N-myc*-deficient retinas. (*D–F*) Representative pictures of adult (P30) eyes with intact lens from control (*N-myc*$^{Lox/Lox}$) (*D*), *N-myc*-deficient (*Nestin-Cre, N-myc*$^{Lox/Lox}$) (*E*), and double-deficient (*Nestin-Cre, N-myc*$^{Lox/Lox}$*;p27Kip1*$^{-/-}$) mice (*F*). (*G*) E14.5 retinal explants were infected with NIN-E retrovirus and maintained in culture for 10 d. Clone size and proportion were then quantified. Clonal analysis revealed that genetic deletion of *p27Kip1* (striped bars; $n = 8$) rescued the impaired cell proliferation of *N-myc*-deficient retinal progenitor cells (filled bars; $n = 8$). (*H*) P0 *N-myc*$^{Lox/Lox}$ retinas were coelectroporated with either a control vector or a vector expressing Cre and with a *p27Kip1* promoter–luciferase vector. After 2 d in culture, retinal explants were lysed and luciferase expression was measured. Acute inactivation of *N-myc* increased *p27Kip1*-driven luciferase expression. (*I*) P0 *N-myc*$^{Lox/Lox}$ retinas were coelectroporated with either a control vector or a vector expressing N-myc (pUB-N-myc) and with a *p27Kip1* promoter–luciferase vector. Overexpression of N-myc decreased *p27Kip1*-driven luciferase expression, indicating that N-myc negatively regulates *p27Kip1* transcription in retinal progenitor cells. Error bars indicate SEM.

retinas (Fig. 6G–L). Real-time RT–PCR analysis using TaqMan probes for cell-type-specific genes confirmed that each retinal cell type was produced normally in the absence of N-myc (Supplemental Fig. 3).

N-myc coordinates retinal progenitor cell proliferation and eye growth

Having found that the adult *N-myc*-deficient mice have smaller hypocellular retinas and impaired retinal progenitor cells proliferation, we tested whether *N-myc* deficiency affected retinal thickness. Adult retinas (P30) from *N-myc*-deficient and control littermates were isolated, and the relative thickness of each cellular layer was measured from sections through the optic nerve (Fig. 7A,B). No significant difference in the relative thickness of any retinal layer was observed in the *N-myc*-deficient retinas (Fig. 7C).

To examine whether the *N-myc*-deficient retina is proportional to the other components of the eye, we determined the relative size of the cornea, anterior chamber, lens, vitreous, and retinas in bisected frozen blocks (Fig.

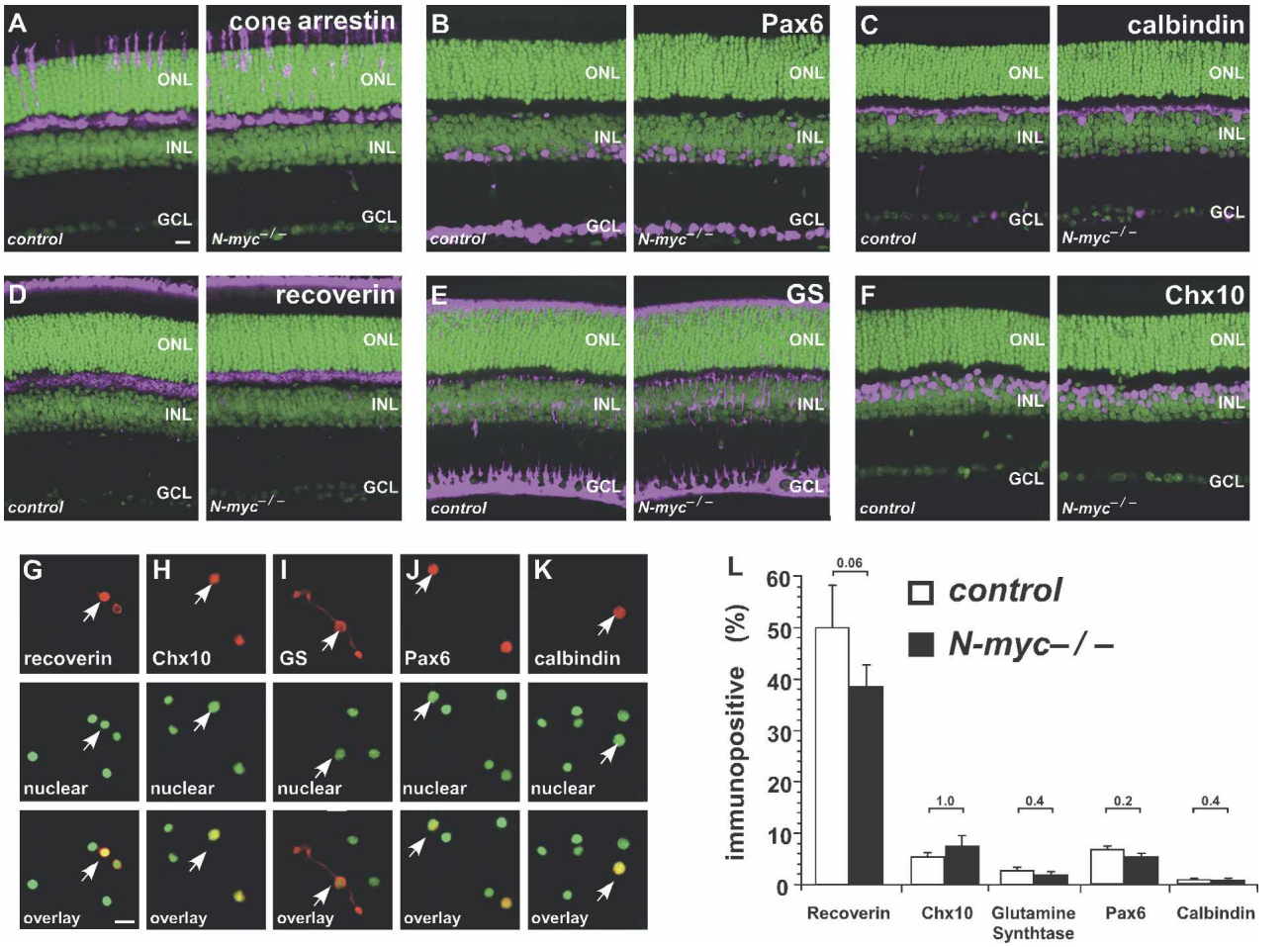

Figure 6. Retinal cell fate specification and differentiation are normal in *N-myc*-deficient retinas. Retinal sections from adult (P30) control (*N-myc*$^{Lox/Lox}$) and *N-myc*-deficient (*Nestin-Cre, N-myc*$^{Lox/Lox}$) mice were prepared on a vibratome (50-µm) and then immunostained with cell-type-specific antibodies. Immunopositive cells are shown in pink, and nuclei are shown in green. Cone arrestin (cone photoreceptors) (*A*), Pax6 (amacrine cells) (*B*), calbindin (horizontal cells) (*C*), recoverin (photoreceptors and a subset of bipolar cells) (*D*), glutamine syntethase (GS, Müller glia) (*E*), and Chx10 (bipolar cells) (*F*) immunostaining patterns are indistinguishable between *N-myc*-deficient and control retinas. To quantitate the proportion of each cell type, we performed immunostaining on dissociated retinas from control and *N-myc*-deficient mice. (*G–K*) Representative pictures of dissociated retinal cells stained with indicated antibodies. Red indicates immunopositive cells, and green indicates nuclear staining. (*L*) The proportion of immunopositive cells for each antibody was determined from five control (open bars) or *N-myc*-deficient (filled bars) mice and no significant difference was detected. (ONL) Outer nuclear layer; (INL) inner nuclear layer; (GCL) ganglion cell layer. Error bars indicate SEM. Bar, 10 µm.

7D–F) as described previously (Remtulla and Hallett 1985). *cyclin D1*-deficient eyes were used as a control, because their retinas are not properly proportioned to the eye size (Ma et al. 1998). Axial length (the sum of cornea, anterior chamber, lens, vitreous, and retinal thicknesses) measurements confirmed that *N-myc*-deficient eyes were significantly smaller than control eyes ($P = 0.009$) (Fig. 7G). Although the volume of *cyclin D1*-deficient retinas was significantly smaller then that of *N-myc*-deficient retinas (Fig. 4G), the axial lengths of *cyclin D1*-deficient and *N-myc*-deficient eyes were indistinguishable (Fig. 7G; Table 2). Measurements of the retinal thickness from whole eye cross-sections confirmed that the thickness of *N-myc*-deficient retinas was the same as that of control retinas (Fig. 7H). The *cyclin D1*$^{-/-}$ retinas (Fig. 7E) were significantly thinner than control retinas ($P = 0.003$) (Fig. 7H; Table 2) even though the eyes were the same size of *Nestin-Cre; N-myc*$^{Lox/Lox}$ eyes. The lens thickness and lens volume were proportional to eye size in the *N-myc*-deficient mice but not in the *cyclin D1*-deficient eyes (Fig. 7I; Table 2).

High expression of c-myc in developing retina suggested a functional role of this Myc family member in eye development (Supplemental Fig. 1). To test this hypothesis, we determined the relative size of ocular structures of *c-myc*-deficient (*Nestin-Cre; N-myc*$^{+/Lox}$*; c-myc*$^{Lox/Lox}$) and *N-myc* and *c-myc* double-knockout mice (*Nestin-Cre; N-myc*$^{Lox/Lox}$*; c-myc*$^{Lox/Lox}$). The volume of the *c-myc*-deficient retinas was significantly smaller than that of the control retinas ($P = 0.03$). Simultaneous

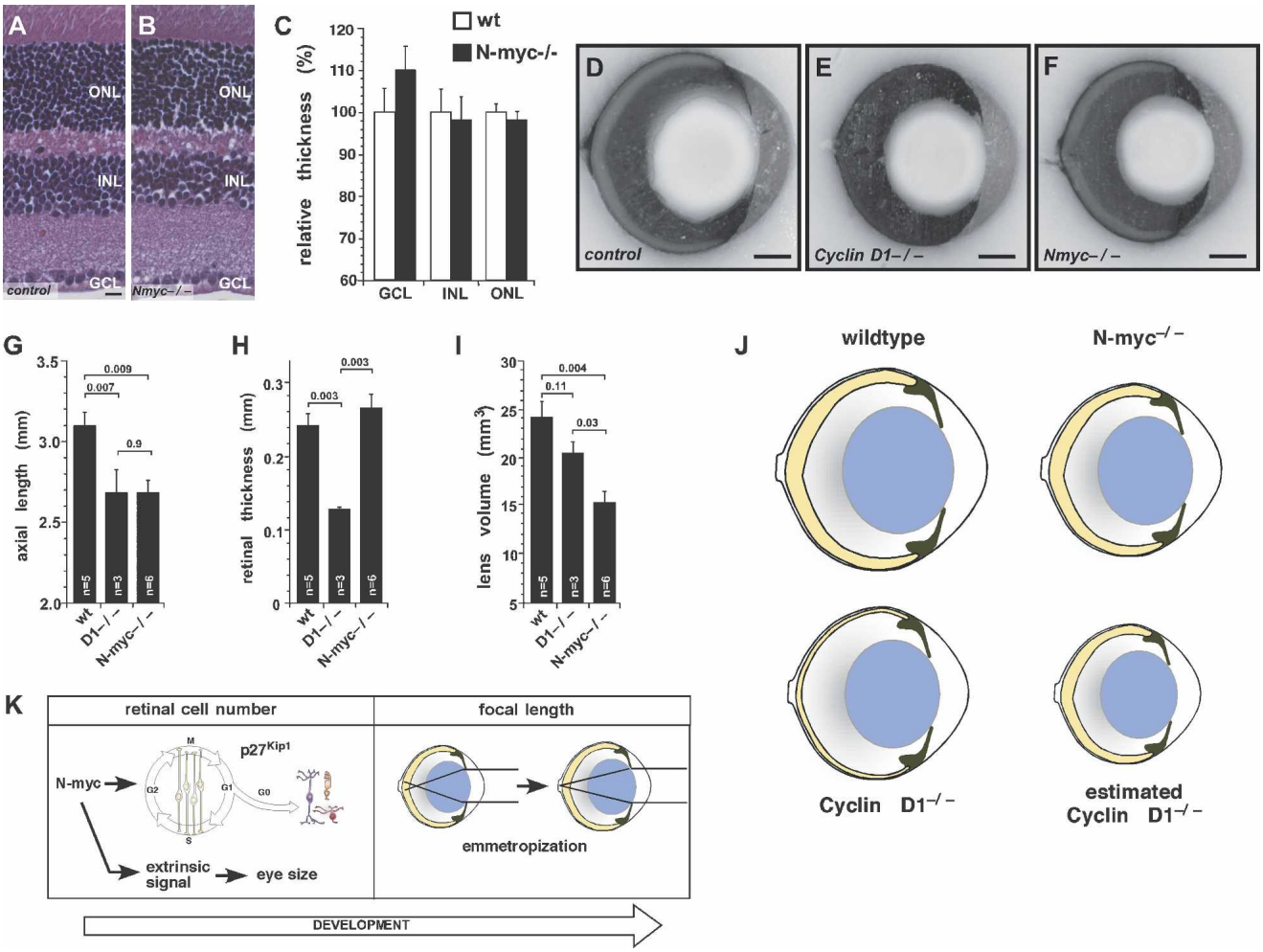

Figure 7. *N-myc* deficiency leads to smaller eyes with unchanged retinal thickness. (*A*,*B*) Representative pictures of H&E-stained paraffin-embedded sections (1 µm) of control (*N-myc*$^{Lox/Lox}$) (*A*) and *N-myc*-deficient (*Nestin-Cre*, *N-myc*$^{Lox/Lox}$) (*B*) adult retinas (P30). (*C*) No difference was detected in the thickness of adult *N-myc*-deficient (filled bars, $n = 12$) and control (open bars, $n = 12$) retinas after measurement of the relative thickness of each nuclear layer (ganglion cell layer [$P = 0.19$], inner nuclear layer [$P = 1.0$], or outer nuclear layer [$P = 0.59$]). (*D–F*) Representative pictures of bisected frozen blocks of adult (P30) eyes from control (*N-myc*$^{Lox/Lox}$) (*D*), *cyclin D1*-deficient (*cyclin D1*$^{-/-}$) (*E*), or *N-myc*-deficient (*Nestin-Cre*, *N-myc*$^{Lox/Lox}$) (*F*) mice. Axial length (sum of the thickness of cornea, anterior chamber, lens, vitreous, and retina) (*G*) and retinal thickness (*H*) were measured on pictures of the bisected frozen eyes. (*I*) Lens volume was calculated after measuring the sagital and coronal axes of adult (P30) lenses of the indicated genotypes. No difference in retinal thickness was observed in the hypocellular *N-myc*-deficient retinas. As observed in wild-type eyes, *N-myc*-deficient retinas were proportional to other eye structures. (*J*) Cartoon shows the relative size of wild-type, *N-myc*-deficient, and *cyclin D1*-deficient eyes and retinas. The estimated cyclin D1 diagram shows how much smaller the eye would need to be to have a proportioned eye and retina. (*K*) We propose a model in which N-myc plays a role in regulating retinal and eye growth during eye development in the absence of visual input. Later, during maturation of the visual system, emmetropization fine-tunes the relative size of ocular structures. (ONL) Outer nuclear layer; (INL) inner nuclear layer; (GCL) ganglion cell layer. Error bars indicate SEM. Bars: *A*,*B*, 10 µm; *D–F*, 0.5 mm.

inactivation *N-myc* and *c-myc* resulted in a greater reduction of retinal volume (Supplemental Fig. 4A–D). Interestingly, inactivation of both genes also led to a sharp decrease in lens volume (Supplemental Fig. 4E) and axial length (Supplemental Fig. 4F–I). However, as observed for *N-myc*-deficient mice, deletion of *N-myc* and *c-myc* did not affect retinal thickness (Supplemental Fig. 4H,J). These data suggest that N-myc and c-myc may cooperatively coordinate retinal to eye growth during development.

Discussion

We found that N-myc is required for proper retinal progenitor cell proliferation in the developing retina. In the absence of N-myc, retinal progenitor cell proliferation is reduced, and the adult retina is hypocellular. N-myc does not play a role in regulating cell survival or neuronal differentiation in the developing mouse retina. Using genetic, molecular, and biochemical assays, we found that N-myc regulates retinal progenitor cell proliferation

Table 2. *Thickness of the optical components of wild-type, cyclin D1-deficient, and N-myc-deficient eyes*

Genotype	Thickness (mm)					
	Axial length	Cornea	Anterior chamber	Lens	Vitreous	Retina
N-myc$^{lox/lox}$	3.10 ± 0.08 (n = 5)	0.10 ± 0.08 (n = 5)	0.44 ± 0.03 (n = 5)	1.65 ± 0.06 (n = 5)	0.60 ± 0.07 (n = 5)	0.24 ± 0.01 (n = 5)
Cyclin D1$^{-/-}$	2.68 ± 0.15 (n = 3)	0.12 ± 0.02 (n = 3)	0.38 ± 0.03 (n = 3)	1.45 ± 0.10 (n = 3)	0.66 ± 0.02 (n = 3)	0.13 ± 0.001 (n = 3)
Nestin-Cre; N-myc$^{lox/lox}$	2.65 ± 0.08 (n = 6)	0.10 ± 0.06 (n = 6)	0.32 ± 0.02 (n = 6)	1.36 ± 0.11 (n = 6)	0.53 ± 0.03 (n = 6)	0.26 ± 0.02 (n = 6)

by influencing the expression of the p27Kip1 CKI. Unlike other tissues that require N-myc for their proper development, in the developing retina, N-myc acts independently of cyclin D1. Acute inactivation of the *N-myc*^{Lox} allele demonstrated that N-myc is required in a cell-autonomous manner for proper retinal progenitor cell proliferation. This represents the first example of a role for Myc family members in retinal development. In addition, inactivation of N-myc in the developing retina led to a hypocellular retina in an eye that was properly proportioned to the smaller retina. *N-myc*-deficient mice are the first genetically engineered mouse with a small eye phenotype in which all of the eye components are properly proportioned. On the basis of these data, we propose that N-myc plays a central role in coordinating retinal proliferation with eye growth during development.

N-myc regulates retinal progenitor cell proliferation

Myc family proteins regulate fundamental cellular processes such as cell proliferation (cell cycle and cell division), cell growth (cell size regulation), cell differentiation, and cell death in a variety of biological systems (for review, see Grandori et al. 2000). For example, cerebellar hypoplasia in *Nestin-Cre; N-myc*$^{Lox/Lox}$ mice is caused by fewer cerebellar progenitor cells and impaired cell division concomitant with neuronal differentiation (Knoepfler et al. 2002). The cerebellar progenitor cells in *N-myc*-deficient mice express higher levels of the *p18Ink4c* and *p27Kip1* CKIs, suggesting that N-myc directly or indirectly regulates the expression of these two genes in the developing cerebellum (Knoepfler et al. 2002). Importantly, the hypoplasia of the *N-myc*-deficient cerebellum is partially rescued by simultaneous inactivation of *p18Ink4c* and *p27Kip1*, demonstrating the functional significance of their increased expression (Zindy et al. 2006).

Our data indicate that N-myc is a cell-autonomous regulator of retinal progenitor proliferation. Acute inactivation studies, lineage analysis, and cell proliferation assays revealed that N-myc negatively regulates progenitor cell proliferation during embryonic and postnatal development. Although no difference in the volume of E12.5 retinas was observed (Fig. 2A), it is possible that in the retina a reduction in the starting population of retinal progenitor cell could also contribute to hypocellularity of *N-myc*-deficient retinas.

In contrast to previous studies in other tissues (Okubo et al. 2005) *N-myc* deficiency did not affect programmed cell death during retinal development. Acute or chronic inactivation of N-myc did not change the proportion or the developmental timing of apoptotic cell death in the retina. Moreover, all cell types were present in the normal position and at the correct proportions. These results suggest that N-myc is required for proper retinal progenitor cell proliferation in the developing mouse retina throughout retinal histogenesis and that it plays no role in cell fate specification, differentiation, or survival of retinal cells.

Regulation of the expression of cell cycle genes by N-myc

Previous work indicated that N-myc may regulate cell proliferation in the developing CNS by controlling the expression of different cyclins (Knoepfler et al. 2002; Kenney et al. 2003; Oliver et al. 2003). No difference in the expression of cyclins D1 or D3 (data not shown) was observed after *N-myc* acute inactivation, and genetic studies using *N-myc; cyclin D1* double-knockout retinas confirmed that N-myc acts independently of cyclin D1 in the developing mouse retina.

Earlier research has established an essential role of p19Ink4d and p27Kip1 in the control of cell cycle exit of retinal progenitor cells (Levine et al. 2000; Dyer and Cepko 2001b; Cunningham et al. 2002). However, little is known about how the expression of those molecules is regulated during retinal development. We present evidence that N-myc negatively regulates the expression of p27Kip1 during retinal development. Acute inactivation of *N-myc* in retinal progenitor cells resulted in increased expression of p27Kip1, and the hypocellular phenotype was rescued in *N-myc; p27Kip1*-deficient retinas. It is not known if N-myc directly represses p27Kip1 transcription in the developing retina or if p27Kip1 mRNA expression is inhibited through an indirect mechanism. Preliminary evidence shows that in both overexpression and acute inactivation assays, N-myc expression differentially regulates the activity of a mouse p27Kip1 promoter-driven luciferase reporter construct. However, post-translational regulation of p27Kip1 by N-myc cannot be ruled out (Nakamura et al. 2003). In addition, N-myc was recently shown to globally regulate chromatin structure and gene expression (Knoepfler et al. 2006), raising the possibility that an epigenetic mechanism underlies the connection between N-myc and p27Kip1 levels in the mouse retina.

N-myc is amplified in a subset of human retinoblastoma tumors (Lee et al. 1984; Choi et al. 1993). Recently, *N-myc* amplification was also shown in mouse models of retinoblastoma (MacPherson et al. 2007). Therefore, the determination of N-myc target genes during retinal development may also contribute to the current understanding of retinoblastoma progression.

N-myc coordination of eye and retinal growth

Proper visual processing depends on the development of an optical system that precisely focuses the light on the outer segments of the photoreceptors. Therefore, the growth of the retina, lens, and other eye components must be coordinated for proper vision. We present a model in which the coordination of the growth of the retina and other eye structures has two key components (Fig. 7K). First, the formation and growth of the ocular structures must be regulated during eye development to ensure that they are properly proportioned. Second, once eye morphogenesis is complete, a process called emmetropization fine-tunes the relative size of ocular structures to properly focus the light on the retina. The growth of the retina and eye structures during development is regulated independent of light input, and emmetropization is dependent on visual input (Norton and Siegwart 1995; Wallman and Winawer 2004).

Our data suggest that N-myc is an important regulator of the growth of ocular structures during eye development. In N-myc-deficient eyes, the retina is hypocellular, but it is precisely proportioned to the size of the eye, and its thickness is indistinguishable from control retinas (Fig. 7J). Similar results were observed for mice with conditional inactivation of both N-myc and c-myc (Supplemental Fig. 4) in which impairment of retinal and eye growth is more pronounced, but retinal thickness is unchanged. In contrast, in cyclin D1-deficient eyes, the retina is too thin for the size of the eye, and the mice are blind (Fig. 7J). With the number of cells that are present in the cyclin D1-deficient retinas, the size of the eye would have to be significantly smaller to produce a retina of the proper thickness (Fig. 7J). This is the first genetic model of decreased retinal progenitor cell proliferation in the developing mouse in which a hypocellular retina is properly coordinated with eye size. There is no relationship between body size and eye size in these mice (data not shown). We propose that extrinsic signals from the retina help coordinate lens and eye growth (Fig. 7K). Signaling molecules, such as FGF and IGF, that are actively produced by developing retina have been shown to regulate the growth of other ocular structures, such as the lens (Cuthbertson et al. 1989; McAvoy et al. 1991; Lovicu and Overbeek 1998; Blackshaw et al. 2004; Xie et al. 2006). Specifically, we hypothesize that N-myc is upstream of those signals such that when N-myc is inactivated, there is a reduction in retinal progenitor cell proliferation and the extrinsic cues that regulate eye growth in concert with retinal growth. (Fig. 7K). In contrast, in mutants such as *Chx10*$^{-/-}$ and *cyclin D1*$^{-/-}$ (Burmeister et al. 1996; Ma et al. 1998; Green et al. 2003), mice that have uncoupled retinal and eye growth, the perturbation lies downstream from this mechanism, thereby resulting in the disproportioned eyes.

Different components of the visual system such as eye size vary across species, but retinal thickness remains relatively constant (Glickstein and Millodot 1970; Remtulla and Hallett 1985). Importantly, for the retinas to maintain nearly constant thickness across species that have different sizes of eyes, the total number of retinal cells must change severalfold. The identification of N-myc as a key regulator of these processes allows us to begin to understand the coordination of complex developmental programs in the developing eye and how these processes have evolved.

Materials and methods

Animals and retinal explant cultures

Mice were obtained as reported previously (Cunningham et al. 2002; Knoepfler et al. 2002; Zindy et al. 2006). Procedures for maintaining mouse retinal explants in culture were also described previously (Dyer and Cepko 2001b).

Volume measurements

Dissected retinas (P7, P15, or adult) or E12.5 eyes were embedded in agar or paraffin, and serial sections were cut on a vibratome or microtome, respectively. Sections of adult tissue were 140 µm thick, and those of embryonic tissue were 4 µm thick. The volumes of the tissues were then reconstructed using BioQuant 5.0 software (BioQuant Image Analysis Corp.).

RNA extraction, cDNA synthesis, and real-time RT–PCR analysis

Retinas were removed from staged embryonic (E14.5, E17.5) and postnatal (P0, P3, P6, P12, adult) mice. RNA extraction and cDNA synthesis were performed as described previously (Martins et al. 2006). Four retinas per sample were harvested for embryonic stages. For adult and postnatal stages, one retina per sample was used.

In situ hybridization

In situ hybridization was performed as described previously (Donovan et al. 2006).

Immunohistochemistry, antibodies, and apoptosis analysis

Immunostaining procedures were done as reported previously (Martins et al. 2006). Antibody dilutions and sources were as follows: BrdU, 1:3 (Amersham Biosciences; #RPN20); Pax6, 1:25 (Developmental Studies Hybridoma Bank); pH3, 1:100 (CST #9701); activated caspase-3, 1:500 (BD PharMingen; #557035); cone arrestin, 1:2000 (from C. Craft); calbindin, 1:2000 (Sigma; #C8666); recoverin, 1:2000 (from J. McGinnis); glutamine synthetase, 1:1000 (BD Biosciences; #G45020); chx10, 1:2000 (Exalpha Biologicals, Inc.; #X1180P). Dissociated cells or retinal sections were stained using the TUNEL apoptosis system (Promega). For detection, we used Cy3-tyramide rather than the colorimetric substrate. For nuclear staining, slides were incubated with either Sytox Green or DAPI, 1:20,000 (Invitrogen).

Images were captured with a Nikon TE2000E2 inverted confocal microscope (Nikon).

BrdU and [^{3}H]-thymidine labeling

S-phase retinal progenitor cells were labeled in explant culture medium containing 10 µM BrdU (Boehringer Mannheim) or [^{3}H]-thymidine (5 µCi/mL; 89 Ci/mmol) for the indicated times. Autoradiographic detection was carried out as described previously (Dyer and Cepko 2001b).

Retroviral labeling and lineage analysis

Retinal progenitor cells were infected with NIN-E or NIN-Cre retrovirus, and their lineage was analyzed as described previously (Dyer and Cepko 2001b). For each mouse, the total number of clones, average number of cells per clone, and the proportion of clones of each size were computed.

Electroporation and FACS

Electroporation of embryonic mouse retinas and FACS purification after explant culture were performed as reported previously (Matsuda and Cepko 2004; Donovan and Dyer 2006; Martins et al. 2006).

Immunoblot analysis

Total retinal protein extraction and immunoblot procedures were performed as reported previously (Martins et al. 2006). Primary antibodies were as follows: cyclin D1 (Santa Cruz Bioctechnology; #2926), p27Kip1 (Cell Signaling Technology; #2552), and N-myc (Abcam; #ab16898). HRP-conjugated secondary antibodies were used at a dilution of 1:1000. The Amersham ECL system was used according to the manufacturer's instructions.

Morphometric measurements of the eye

Eyes from adult mice (P30) were processed as described previously (Remtulla and Hallett 1985). In brief, eyes were removed and rapidly frozen in embedding media. Sagittal sections were cut on a cryostat until the axis of greatest eye diameter was reached, as indicated by the appearance of the optic nerve. Pictures were acquired, and the thickness of each component of the eye was measured. For cell density measurements, adult (P30) eyes were embedded in paraffin, and sections (1 µm thick) of the central region of the eye were stained with hematoxylin and eosin. The number of nuclei per area was determined for each nuclear layer using using Metamorph software. Each field was 450 µm^2, and six independent fields were scored for each retina. For each genotype, the number of animals analyzed was three.

Statistical analysis

For lineage analysis, the proportion of clones of different sizes was computed for each mouse. The exact Kruskal-Wallis test was used to compare the medians across all groups, and the exact rank-sum test was used to perform pairwise comparisons of medians (Pounds and Dyer 2007). For all other experiments, samples were tested (Shapiro-Wilks test) to determine if they would fit to a normal distribution. Analysis by general linear models was used in normally distributed data sets. Other comparisons were performed using the rank-sum or Kruskal-Wallis test. In a few cases with a very large number of possible permutations, a Monte-Carlo approximation based on 10,000 permutations was used to compute the *P*-value for the Kruskal-Wallis test. *P*-values are based on two-sided tests. The exact Kruskal-Wallis test was performed using SAS software (SAS Institute), and the exact rank-sum test was performed using R software (http://www.r-project.org).

Acknowledgments

We thank Dianna Johnson for advice about morphometric measurements; Barbara Finlay for helpful discussions; Angie McArthur for editing the manuscript; Marina Kedrov, Shelly Wilkerson, and Yun Jiao for technical support; and Dr. Phillip Koeffler for providing the p27Kip1 promoter–luciferase construct. This work was supported by grants from the National Institutes of Health, Cancer Center Support from the National Cancer Institute, Research to Prevent Blindness, the American Cancer Society, the Pearle Vision Foundation, and the American Lebanese Syrian Associated Charities (ALSAC). M.A.D. is a Pew Scholar.

References

Aldosari, N., Bigner, S.H., Burger, P.C., Becker, L., Kepner, J.L., Friedman, H.S., and McLendon, R.E. 2002. MYCC and MYCN oncogene amplification in medulloblastoma. A fluorescence in situ hybridization study on paraffin sections from the Children's Oncology Group. *Arch. Pathol. Lab. Med.* **126:** 540–544.

Alexiades, M.R. and Cepko, C. 1996. Quantitative analysis of proliferation and cell cycle length during development of the rat retina. *Dev. Dyn.* **205:** 293–307.

Blackshaw, S., Fraioli, R.E., Furukawa, T., and Cepko, C. 2001. Comprehensive analysis of photoreceptor gene expression and the identification of candidate retinal disease genes. *Cell* **107:** 579–589.

Blackshaw, S., Harpavat, S., Trimarchi, J., Cai, L., Huang, H., Kuo, W., Weber, G., Lee, K., Fraioli, R.E., Cho, S.H., et al. 2004. Genomic analysis of mouse retinal development. *PLoS Biol.* **2:** E247. doi: 10.1371/journal.pbio.0020247.

Brodeur, G.M., Seeger, R.C., Schwab, M., Varmus, H.E., and Bishop, J.M. 1984. Amplification of N-myc in untreated human neuroblastomas correlates with advanced disease stage. *Science* **224:** 1121–1124.

Burmeister, M., Novak, J., Liang, M.Y., Basu, S., Ploder, L., Hawes, N.L., Vidgen, D., Hoover, F., Goldman, D., Kalnins, V.I., et al. 1996. Ocular retardation mouse caused by *Chx10* homeobox null allele: Impaired retinal progenitor proliferation and bipolar cell differentiation. *Nat. Genet.* **12:** 376–384.

Cepko, C.L., Austin, C.P., Yang, X., Alexiades, M., and Ezzeddine, D. 1996. Cell fate determination in the vertebrate retina. *Proc. Natl. Acad. Sci.* **93:** 589–595.

Charron, J., Malynn, B.A., Fisher, P., Stewart, V., Jeannotte, L., Goff, S.P., Robertson, E.J., and Alt, F.W. 1992. Embryonic lethality in mice homozygous for a targeted disruption of the N-*myc* gene. *Genes & Dev.* **6:** 2248–2257.

Choi, S.W., Lee, T.W., Yang, S.W., Hong, W.S., Kim, C.M., and Lee, J.O. 1993. Loss of retinoblastoma gene and amplification of N-myc gene in retinoblastoma. *J. Korean Med. Sci.* **8:** 73–77.

Cole, M.D. and Nikiforov, M.A. 2006. Transcriptional activation by the Myc oncoprotein. *Curr. Top. Microbiol. Immunol.* **302:** 33–50.

Cunningham, J.J., Levine, E.M., Zindy, F., Goloubeva, O., Rous-

sel, M.F., and Smeyne, R.J. 2002. The cyclin-dependent kinase inhibitors $p19^{Ink4d}$ and $p27^{Kip1}$ are coexpressed in select retinal cells and act cooperatively to control cell cycle exit. *Mol. Cell. Neurosci.* **19:** 359–374.

Cuthbertson, R.A., Beck, F., Senior, P.V., Haralambidis, J., Penschow, J.D., and Coghlan, J.P. 1989. Insulin-like growth factor II may play a local role in the regulation of ocular size. *Development* **107:** 123–130.

Davis, A.C., Wims, M., Spotts, G.D., Hann, S.R., and Bradley, A. 1993. A null c-*myc* mutation causes lethality before 10.5 days of gestation in homozygotes and reduced fertility in heterozygous female mice. *Genes & Dev.* **7:** 671–682.

Donovan, S.L. and Dyer, M.A. 2006. Preparation and square wave electroporation of retinal explant cultures. *Nat. Protoc.* **1:** 2710–2718.

Donovan, S.L., Schweers, B., Martins, R., Johnson, D., and Dyer, M.S. 2006. Compensation by tumor suppressor genes during retinal development in mice and humans. *BMC Biol.* **4:** 14.

Dyer, M.A. and Cepko, C. 2001a. Regulating proliferation during retinal development. *Nat. Rev. Neurosci.* **2:** 333–342.

Dyer, M.A. and Cepko, C. 2001b. $p27^{Kip1}$ and $p57^{Kip2}$ regulate proliferation in distinct retinal progenitor cell populations. *J. Neurosci.* **21:** 4259–4271.

Eisenman, R.N. 2001. Deconstructing myc. *Genes & Dev.* **15:** 2023–2030.

ElShamy, W.M., Fridvall, L.K., and Ernfors, P. 1998. Growth arrest failure, G1 restriction point override, and S phase death of sensory precursor cells in the absence of neurotrophin-3. *Neuron* **21:** 1003–1015.

Glickstein, N. and Millodot, M. 1970. Retinoscopy and eye size. *Science* **168:** 605–606.

Grandori, C., Cowley, S.M., James, L.P., and Eisenman, R.N. 2000. The Myc/Max/Mad network and the transcriptional control of cell behavior. *Annu. Rev. Cell Dev. Biol.* **16:** 653–699.

Graus-Porta, D., Blaess, S., Senften, M., Littlewood-Evans, A., Damsky, C., Huang, Z., Orban, P., Klein, R., Schittny, J.C., and Muller, U. 2001. β1-class integrins regulate the development of laminae and folia in the cerebral and cerebellar cortex. *Neuron* **31:** 367–379.

Green, E., Stubbs, J., and Levine, E.M. 2003. Genetic rescue of cell number in a mouse model of microphthalmia: Interactions between Chx10 and G1-phase cell cycle regulators. *Development* **130:** 539–552.

Hatton, B.A., Knoepfler, P.S., Kenney, A.M., Rowitch, D.H., de Alboran, I.M., Olson, J.M., and Eisenman, R.N. 2006. N-*myc* is an essential downstream effector of Shh signaling during both normal and neoplastic cerebellar growth. *Cancer Res.* **66:** 8655–8661.

Kenney, A.M., Cole, M.D., and Rowitch, D.H. 2003. *Nmyc* upregulation by sonic hedgehog signaling promotes proliferation in developing cerebellar granule neuron precursors. *Development* **130:** 15–28.

Kleine-Kohlbrecher, D., Adhikary, S., and Eilers, M. 2006. Mechanisms of transcriptional repression by Myc. *Curr. Top. Microbiol. Immunol.* **302:** 51–62.

Knoepfler, P.S., Cheng, P.R., and Eisenman, R.N. 2002. N-*myc* is essential during neurogenesis for the rapid expansion of progenitor cell populations and the inhibition of neuronal differentiation. *Genes & Dev.* **16:** 2699–2712.

Knoepfler, P.S., Zhang, X.Y., Cheng, P.F., Gafken, P.R., McMahon, S.B., and Eisenman, R.N. 2006. Myc influences global chromatin structure. *EMBO J.* **25:** 2723–2734.

Lee, W.H., Murphree, A.L., and Benedict, W.F. 1984. Expression and amplification of the N-myc gene in primary retinoblastoma. *Nature* **309:** 458–460.

Levine, E.M., Close, J., Fero, M., Ostrovsky, A., and Reh, T.A. 2000. $p27^{Kip1}$ regulates cell cycle withdrawal of late multipotent progenitor cells in the mammalian retina. *Dev. Biol.* **219:** 299–314.

Livesey, F.J. and Cepko, C.L. 2001. Vertebrate neural cell-fate determination: Lessons from the retina. *Nat. Rev. Neurosci.* **2:** 109–118.

Lovicu, F.J. and Overbeek, P.A. 1998. Overlapping effects of different members of the FGF family on lens fiber differentiation in transgenic mice. *Development* **125:** 3365–3377.

Lutz, W., Leon, J., and Eilers, M. 2002. Contributions of Myc to tumorigenesis. *Biochim. Biophys. Acta* **1602:** 61–71.

Ma, C., Papermaster, D., and Cepko, C.L. 1998. A unique pattern of photoreceptor degeneration in *cyclin D1* mutant mice. *Proc. Natl. Acad. Sci.* **95:** 9938–9943.

McAvoy, J.W., Chamberlain, C.G., de Iongh, R.U., Richardson, N.A., and Lovicu, F.J. 1991. The role of fibroblast growth factor in eye lens development. *Ann. N. Y. Acad. Sci.* **638:** 256–274.

MacPherson, D., Sage, J., Kim, T., Ho, D., McLaughlin, M.E., and Jacks, T. 2004. Cell type-specific effects of *Rb* deletion in the murine retina. *Genes & Dev.* **18:** 1681–1694.

MacPherson, D., Conkrite, K., Tam, M., Mukai, S., Mu, D., and Jacks, T. 2007. Murine bilateral retinoblastoma exhibiting rapid-onset, metastatic progression and *N-myc* gene amplification. *EMBO J.* **26:** 784–794.

Martins, R.A., Linden, R., and Dyer, M.A. 2006. Glutamate regulates retinal progenitors cells proliferation during development. *Eur. J. Neurosci.* **24:** 969–980.

Matsuda, T. and Cepko, C.L. 2004. Electroporation and RNA interference in the rodent retina in vivo and in vitro. *Proc. Natl. Acad. Sci.* **101:** 16–22.

Nakamura, M., Matsuo, T., Stauffer, J., Neckers, L., and Thiele, C.J. 2003. Retinoic acid decreases targeting of p27 for degradation via an N-myc-dependent decrease in p27 phosphorylation and an N-myc-independent decrease in Skp2. *Cell Death Differ.* **10:** 230–239.

Nesbit, C.E., Tersak, J.M., and Prochownik, E.V. 1999. *MYC* oncogenes and human neoplastic disease. *Oncogene* **18:** 3004–3016.

Norton, T.T. and Siegwart Jr., J.T. 1995. Animal models of emmetropization: Matching axial length to the focal plane. *J. Am. Optom. Assoc.* **66:** 405–414.

Okubo, T., Knoepfler, P.S., Eisenman, R.N., and Hogan, B.L. 2005. *Nmyc* plays an essential role during lung development as a dosage-sensitive regulator of progenitor cell proliferation and differentiation. *Development* **132:** 1363–1374.

Oliver, T.G., Grasfeder, L.L., Carroll, A.L., Kaiser, C., Gillingham, C.L., Lin, S.M., Wickramasinghe, R., Scott, M.P., and Wechsler-Reya, R.J. 2003. Transcriptional profiling of the Sonic hedgehog response: A critical role for N-myc in proliferation of neuronal precursors. *Proc. Natl. Acad. Sci.* **100:** 7331–7336.

Pounds, S. and Dyer, M.A. 2007. Statistical analysis of data from retroviral clonal experiments in the developing retina. *Brain Res.* doi: 10.1016/j.brainres.2007.08.074.

Remtulla, S. and Hallett, P.E. 1985. A schematic eye for the mouse, and comparisons with the rat. *Vision Res.* **25:** 21–31.

Schweers, B.A. and Dyer, M.A. 2005. Perspective: New genetic tools for studying retinal development and disease. *Vis. Neurosci.* **22:** 553–560.

Sicinski, P., Donaher, J.L., Parker, S.B., Li, T., Fazeli, A., Gardner, H., Haslam, S.Z., Bronson, R.T., Elledge, S.J., and Weinberg, R.A. 1995. Cyclin D1 provides a link between development and oncogenesis in the retina and breast. *Cell* **82:** 621–630.

Stanton, B.R., Perkins, A.S., Tessarollo, L., Sassoon, D.A., and Parada, L.F. 1992. Loss of N-myc function results in embryonic lethality and failure of the epithelial component of the embryo to develop. *Genes & Dev.* **6:** 2235–2247.

Tronche, F., Kellendonk, C., Kretz, O., Gass, P., Anlag, K., Orban, P.C., Bock, R., Klein, R., and Schutz, G. 1999. Disruption of the glucocorticoid receptor gene in the nervous system results in reduced anxiety. *Nat. Genet.* **23:** 99–103.

Wallman, J. and Winawer, J. 2004. Homeostasis of eye growth and the question of myopia. *Neuron* **43:** 447–468.

Wartiovaara, K., Barnabe-Heider, F., Miller, F., and Kaplan, D. 2002. N-myc promotes survival and induces S-phase entry of postmitotic sympathetic neurons. *J. Neurosci.* **22:** 815–824.

Xie, L., Overbeek, P.A., and Reneker, L.W. 2006. Ras signaling is essential for lens cell proliferation and lens growth during development. *Dev. Biol.* **298:** 403–414.

Yang, W., Shen, J., Wu, M., Arsura, M., FitzGerald, M., Suldan, Z., Kim, D.W., Hofmann, C.S., Pianetti, S., Romieu-Mourez, R., et al. 2001. Repression of transcription of the *p27^{Kip1}* cyclin-dependent kinase inhibitor gene by c-Myc. *Oncogene* **20:** 1688–1702.

Zeller, K.I., Jegga, A.G., Aronow, B.J., O'Donnell, K.A., and Dang, C.V. 2003. An integrated database of genes responsive to the Myc oncogenic transcription factor: Identification of direct genomic targets. *Genome Biol.* **4:** R69. doi: 10.1186/gb-2003-4-10-r69.

Zindy, F., Knoepfler, P.S., Xie, S., Sherr, C.J., Eisenman, R.N., and Roussel, M.F. 2006. N-*Myc* and the cyclin-dependent kinase inhibitors p18^{Ink4c} and p27^{Kip1} coordinately regulate cerebellar development. *Proc. Natl. Acad. Sci.* **103:** 11579–11583.